

# Ischemia Leads to Apoptosis—and Necrosis-like Neuron Death in the Ischemic Rat Hippocampus

Georg Johannes Müller<sup>1</sup>; Christine Stadelmann<sup>2</sup>; Lone Bastholm<sup>3</sup>; Folmer Elling<sup>3</sup>; Hans Lassmann<sup>4</sup>; Flemming Fryd Johansen<sup>1</sup>

<sup>1</sup> Molecular Neuropathology Group, <sup>3</sup>Institute of Molecular Pathology, University of Copenhagen, Denmark.

<sup>2</sup> Institute of Neuropathology, University of Göttingen, Germany.

<sup>4</sup> Brain Research Institute, Medical University of Vienna, Austria.

Corresponding author:

Flemming Fryd Johansen, MD, DMSc, 11, Frederik V vej, DK-2100, Copenhagen, Denmark (E-mail: ffj@nepa.ku.dk)

**Morphological evidence of apoptosis in transient forebrain ischemia is controversial. We therefore investigated the time sequence of apoptosis-related antigens by immunohistochemistry and correlated it with emerging nuclear patterns of cell death in a model of transient forebrain ischemia in CA1 pyramidal cells of the rat hippocampus. The earliest ischemic changes were found on day 2 and 3, reflected by an upregulation of phospho-c-Jun in a proportion of morphologically intact CA1 neurons, which matched the number of neurons that succumbed to ischemia at later time points. At day 3 and later 3 ischemic cell death morphologies became apparent: pyknosis, apoptosis-like cell death and necrosis-like cell death, which were confirmed by electron microscopy. Activated caspase-3 was present in the vast majority of cells with apoptosis-like morphology as well as in a small subset of cells undergoing necrosis; its expression peaked on days 3 to 4. Silver staining for nucleoli, which are a substrate for caspase-3, revealed a profound loss of nucleoli in cells with apoptosis-like morphology, whereas cells with necrosis-like morphology showed intact nucleoli. Overall, cells with apoptosis-like morphology and/or caspase-3 expression represented a minor fraction (<10%) of ischemic neurons, while the vast majority followed a necrosis-like pathway. Our studies suggest that CA1 pyramidal cell death following transient forebrain ischemia may be initiated through c-Jun N-terminal kinase (JNK) pathway activation, which then either follows an apoptosis-like cell death pathway or leads to secondary necrosis.**

*Brain Pathol* 2004;14:415-424.

## INTRODUCTION

The hippocampal formation is one of the most vulnerable brain regions to cerebral ischemia with selective damage in CA1 pyramidal cells (34) and hilar somatostatinergic neurons (29). The mechanism of ischemic CA1 pyramidal cell death is controversial. Initial reports have presumed that ischemic cell death is a form of necrosis, but more recently the importance of apoptosis has been stressed (45). Ischemic CA1 pyramidal cell death both in rodents (33, 47) and humans (26, 46) is characterized by a selective neuronal loss that typically occurs over a 24-72 hours period. This phenomenon is known as “delayed neuronal death” (33) or “maturation phenomenon” (27). The selective ischemic vulnerability of CA1 pyramidal cells and their delayed death have drawn attention to this specific cell type as a candidate for apoptotic cell death. Subsequently, this concept

has mainly been supported by studies based on biochemical criteria. However, the morphology of ischemic cell death in CA1 is not classically apoptotic, when compared with the distinct morphological changes occurring during apoptotic cell death (32, 56). In contrast, ischemic CA1 pyramidal cells do not die by typical necrosis either, as they show only mild cytoplasmic swelling, with or without microvacuolation, followed by moderate shrinkage of cytoplasm and nuclei. Electron microscopic (EM) studies (8, 10) have, based on morphological evidence, argued against apoptosis in CA1 after ischemia in gerbils. However, one EM study in rats (59) showed that a small portion of CA1 neurons, characterized by chromatin condensation and shrinkage of nuclei and cytoplasm, displayed major features of apoptosis. The changes observed were quite different from the picture of

necrosis, which is characterized by pronounced cytoplasmic and organellar swelling, before membrane rupture. These dying neurons have probably not been identified as apoptotic previously because no apoptotic bodies are formed (10, 59).

Programmed cell death (PCD) has been defined as an active process involving signaling mechanisms, ultimately causing death of the cell, whereas apoptosis refers to the morphology of a PCD subtype most likely produced by caspase activation (for review, see 28, 36, 39). In ischemic CA1 pyramidal cells, the lack of classic apoptosis does not exclude the activation of death programs prior to cell death (36). In a number of studies ischemic damage was attenuated by caspase inhibition (7, 11, 17, 24). In order to bridge biochemical evidence of apoptosis and cell death morphologies, we performed quantitative immunohistochemistry of cell death markers in CA1 pyramidal cells of the ischemic rat hippocampus and correlated the immunoreactivity (IR) with ischemic nuclear morphologies of CA1 pyramidal cells in the light microscope (LM). For this purpose we used serial sections of the dorsal hippocampus from rats subjected to transient forebrain ischemia, which were allowed to survive 1, 2, 3, 4, 5 or 7 days. Nuclear morphologies were classified as either *i*) intact, *ii*) shrinkage with hyperchromatism but lack of fragmentation (pyknotic), *iii*) clumped into large round chromatin fragments (apoptosis-like death), or *iv*) fragmented into numerous fine chromatin speckles (necrosis-like death). As markers for apoptosis we used an antibody against activated caspase-3 and an antibody against apoptosis-specific protein (ASP; also termed c-Jun/AP-1, Ab-2). Both antibodies have previously been reported

to label neurons with morphological criteria of apoptosis (14, 16, 31, 51, 52, 53). Nucleoli are a substrate for caspase-3 during apoptosis (25). We therefore performed silver stainings for detection of nucleolar components as a footprint for caspase-3 activity (argyrophilic nucleolin and B23). In addition, we performed immunohistochemistry against phospho-c-Jun (p-c-Jun) as an indicator of early upstream PCD events. In situ tailing (IST) was performed for detection of DNA-fragmentation and irreversible cell damage. Plasma membrane integrity remains intact throughout apoptosis. Therefore, we performed immunohistochemistry against serum albumin to detect loss of plasma membrane integrity and subsequent accumulation of extravasated serum albumin in necrotic neurons. Electron microscopy (EM) was performed of neurons with apoptosis-like and necrosis-like morphology identified in the LM. Using this spectrum of histological markers, we determined the temporal post-ischemic development of apoptosis-like and/or necrosis-like changes with special reference to nuclear LM morphology in the rat hippocampal CA1 pyramidal cell layer.

## MATERIALS AND METHODS

**Cerebral ischemia.** The study was conducted on adult male Wistar rats (Taconic M&B, Ry, Denmark) weighing 300 to 350 g. Ten minutes of transient forebrain ischemia was induced by means of 2-vessel occlusion (50) during systemic hypotension (mean arterial blood pressure, 55 mmHg) as described before (2). Briefly, rats were fasted overnight with free access to water. The following day they were anesthetized with a mixture of 1% halothane in  $O_2/N_2O$  (30%/70%). The left femoral artery was cannulated for continuous control of blood pressure, induction of hypotension, as well as for intermittent sampling of arterial blood (50). Both carotid arteries were gently exposed during anesthesia. Anesthesia was then discontinued for 2 minutes before the common carotid arteries were ligated for 10 minutes. Hypotension was induced immediately before induction of ischemia by withdrawing blood into a heparinized syringe and was maintained throughout the ischemic period. Reperfusion was established by infusion of the extracted blood when the carotid clamps were removed at

the end of the ischemic period. Rats were allowed to survive for 1 (n = 5), 2 (n = 4), 3 (n = 9), 4 (n = 6), 5 (n = 7) and 7 (n = 5) days, respectively. Body core temperature was monitored throughout the surgery and 15 minutes after blood flow was re-established and kept at 37°C. Control rats (n = 4) were sham-operated and kept under identical conditions. Additional rats were subjected to the same ischemia protocol and allowed to survive for 3 (n = 4) and 5 (n = 4) days for studies in the EM.

All animal experiments were performed in accordance with the guidelines of the Danish National Committee on Animal Research Ethics and the European Communities Council Directive #86/609 for the Care of Laboratory Animals.

**Histology.** For perfusion-fixation, animals were deeply anesthetized with 4% halothane in  $N_2O/O_2$  (70%/30%) and perfused transcardially with 4% paraformaldehyde in 0.15 M phosphate buffer (PB, pH 7.3 at 4°C). Brains were postfixed in the same fixative for 4 hours at room temperature (RT) before they were processed for paraffin embedding. Series of coronal sections (~3  $\mu$ m) from the ischemia vulnerable part of the dorsal hippocampus (~3.5 mm caudal to bregma) were cut on a microtome. Serial sections were then processed for hematoxylin and eosin (H&E) staining, for immunohistochemistry against the various antigens, or for in situ tailing (IST). One series of sections was silver stained according to a protocol recognizing nucleoli (38).

**Electron microscopy.** Additional animals were perfusion-fixed with 70% Karnowsky for EM and tissues from the dorsal CA1 hippocampus were postfixed in osmium, dehydrated and embedded in Epon according to standard procedures. Areas showing apoptosis-like and necrosis-like morphologies were identified in one- $\mu$ m thick toluidine-blue stained sections and the pertinent ultra-thin sections were processed for examination in a JEOL1210 electron microscope.

**Tissue stainings.** Immunohistochemistry was performed applying the following antibodies: a rabbit polyclonal antibody against activated caspase-3 (CM1, IDUN Pharmaceuticals, La Jolla, Calif), a rabbit poly-

clonal antibody against ASP (c-Jun/AP-1, Ab-2; Oncogene, Cambridge, Mass), a rabbit polyclonal antibody against albumin (DAKO, Glostrup, Denmark), a mouse monoclonal antibody against glial fibrillary acidic protein (GFAP) (Boehringer Ingelheim, Germany), a rabbit polyclonal antibody against p-c-Jun (Ser63) (Cell Signaling, Beverly, Mass) and a mouse monoclonal antibody against activated microglia (ED1, Serotec, Oxford, United Kingdom). Briefly, sections were dewaxed and antigens recognized by anti-caspase-3 and ASP antibodies were retrieved by microwave 3  $\times$  5 minute in 10 mM citrate buffer, pH 6.0, while sections for GFAP, ED1 and p-c-Jun detection were boiled 60 minutes in a domestic kitchen steamer in the same buffer. After sections had cooled, they were transferred into 10% fetal calf serum (FCS) in 0.12 M phosphate buffered saline (PBS), pH 7.3 (FCS/PBS) at RT to block background staining before applying the primary antibodies. Primary antibodies were applied overnight at 4°C at concentrations of 1:1500 for caspase-3, 1:75 ASP, 1:600 albumin, 1:3000 GFAP, 1:1000 ED1 and 1:50 p-c-Jun in 10% FCS/PBS. Antibody binding was visualized by using a standard avidin-biotin-peroxidase method with 3,3-diaminobenzidine tetrahydrochloride (DAB) as chromogen. Control sections were incubated with FCS/PBS, but without primary antibodies. In order to visualize changed nuclear morphology, all immunostained sections were counterstained with H&E before they were coverslipped with Eukitt®.

IST was performed as described elsewhere (20). Briefly, this method is characterized by a terminal-transferase mediated incorporation of digoxigenin-labeled oligonucleotides at locations of DNA strand breaks, which then are visualized by an anti-digoxigenin antibody.

Silver stainings detecting the argyrophilic nucleolar organizer region (AgNOR) associated proteins (nucleolin and B23) were performed as described previously (38). Briefly, sections were dewaxed, transferred to distilled water and then incubated for 10 minutes with 1% dithiotreitol followed by 3  $\times$  5-minute rinses in distilled water. A freshly prepared 50% aqueous  $AgNO_3$  solution was then blended (2:1) with a 2% aqueous gelatin solution containing 1% formic acid. The solution was dropped

on the slides before they were covered with Parafilm® and placed in a dark humid chamber for 30 minutes. Three times 5-minute rinses followed before the sections were transferred to a 5% aqueous Na<sub>2</sub>S<sub>2</sub>O<sub>3</sub> solution for 5 minutes. Finally, the sections were counterstained with methylgreen, dehydrated and coverslipped with Pertex®.

**Quantitative morphometry.** Numbers of nuclear morphologies and immunopositive CA1 neurons were determined in 17.5 microscopic fields (95 µm each; 17.5×95 µm = 1.66 mm, ~one CA1 counting unit) in sections from ischemic and control animals, throughout the latero-median extent of the CA1 pyramidal cell layer: *i*) cells with intact nuclear morphology, *ii*) cells with pyknotic nuclear changes, *iii*) cells with apoptosis-like nuclear changes, and *iv*) cells with necrosis-like nuclear changes were identified in H&E-stained sections, in immunostained sections and in silver stained sections. About 400 CA1 pyramidal cells were analyzed per section at ×400 magnification. Values represent the number of cells identified with specific nuclear morphologies (H&E-staining, silver staining) and the number of immunopositive cells co-localized with specific nuclear morphologies in 1.66 mm (one counting unit) of the CA1 pyramidal cell layer in one randomly chosen hemisphere at the coronal level -3.5 mm caudal to bregma. For statistical analysis we used the Spearman Rank Order Test. Statistical significance was accepted for  $p < 0.05$ .

## RESULTS

**Ischemic nuclear pathologies.** Based on light microscopic nuclear morphologies at day 1 to 7 after ischemia, CA1 pyramidal cells were classified into neurons with apparently intact nuclei and neurons with shrunken nucleus (ischemic). The latter showed moderate cytoplasmic and nuclear shrinkage and could further be subdivided into nuclear morphologies displaying hyperchromatism without signs of fragmentation (pyknosis), nuclear clumping into large round fragments (apoptosis-like death) and fragmentation of chromatin into speckles (necrosis-like death) (Figure 1).

The earliest ischemic changes appeared one day after ischemia, when 3 to 11 pyknotic neurons appeared per hippocampus.

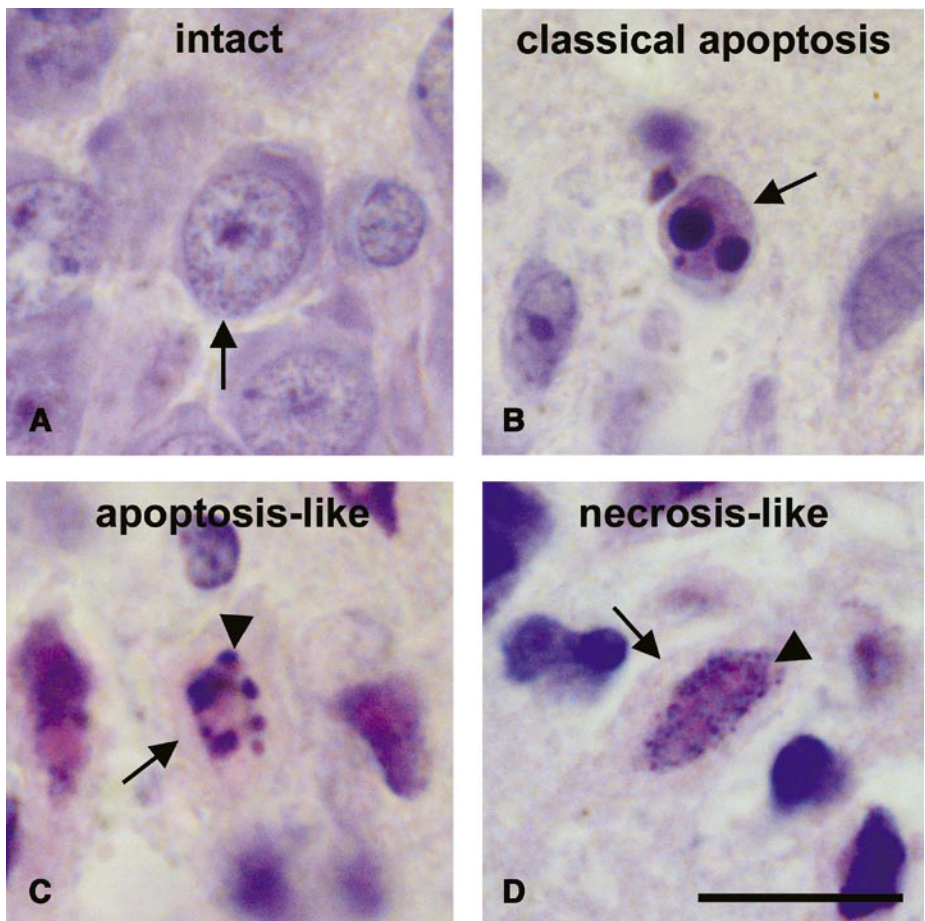


**Figure 1.** Morphologies identified in CA1 pyramidal cells from sham-operated rats (A) and rats surviving 1-7 days after ischemia (B-D). **A.** An intact neuron is shown (arrow). **B.** Classical apoptosis in a neuron with intense shrinkage and strongly condensed chromatin (arrow). Note, no obvious distinction can be made between cytoplasm and nucleoplasm. **C.** Neuron with moderate cytoplasmic and nuclear shrinkage and marked chromatin condensation into large round fragments, termed apoptosis-like (arrow head). An eosinophilic rim of cytoplasm can clearly be detected around the nuclear organization of chromatin fragments (arrow). **D.** Neuron displaying chromatin fragmentation into numerous fine speckles, termed necrosis-like (arrow head), surrounded by an eosinophilic rim of cytoplasm (arrow). Bar: 10 µm.

This low incidence of pyknotic neurons was constant throughout days 1 to 7. After 3 days a small number of CA1 neurons showed either pyknosis, apoptosis-like death or necrosis-like death (Figure 2D). Pyknotic nuclei stained strongly basophilic. In most pyknotic cells, the nuclei appeared triangular-shaped and elongated. Ischemic eosinophilia in cytoplasm was generally seen in the pyknotic neurons and to a lesser extent also in neurons with apoptosis-like death and necrosis-like death. The highest incidence of apoptosis-like death was found at day 4 (Figure 3); however, the highest relative incidence of neurons with apoptosis-like death was found at day 3 (Figure 2E). At day 4 after ischemia, the necrosis-like nuclear morphology was dominant (Figures 2F, 3), but apoptosis-like death could still be seen. At day 5 after ischemia,

the necrosis-like morphology became even more dominant with finer nuclear fragmentation than at day 4 (Figures 2F, 3). Chromatin fragments were evenly distributed throughout the nucleus sparing 1 to 3 round eosinophilic structures (most likely nucleoli). At day 7 after ischemia, the relative distribution of nuclear morphologies in CA1 was similar to that seen 5 days after ischemia (Figure 2). In general, apoptotic crescents and apoptotic bodies were rarely detected. In all ischemic animals, a total of 17 spots with apoptotic bodies were found between days 3 to 7 when in total 9584 ischemic and intact neurons were examined (data not shown).

The incidence of neurons displaying apoptosis-like death and necrosis-like death in each survival group, respectively, is shown in Figure 3 together with the

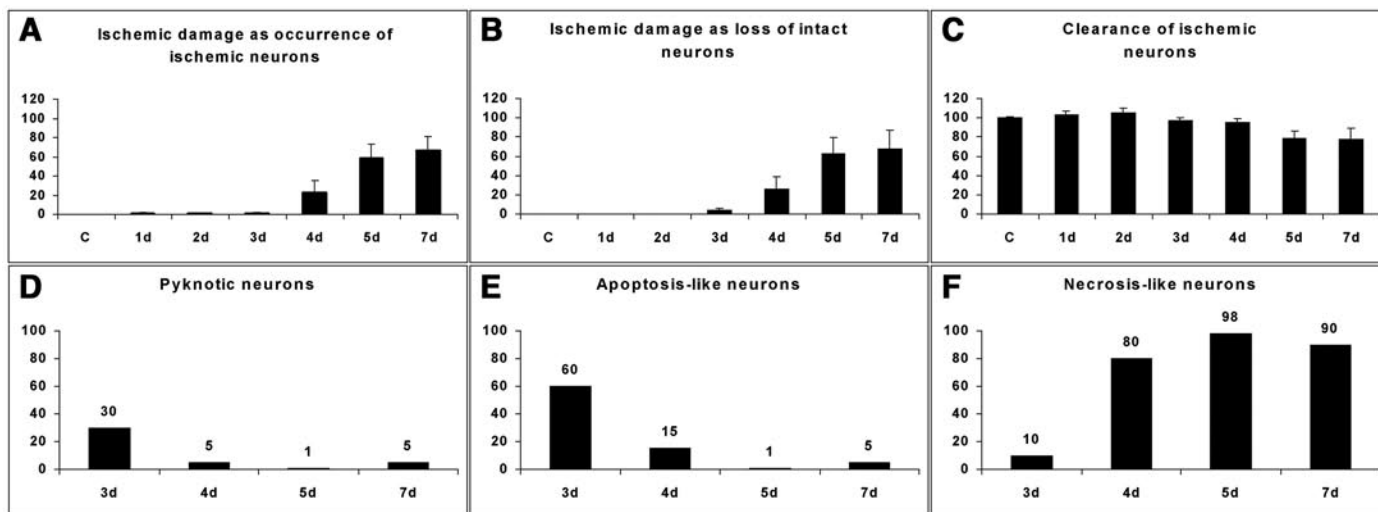


**Figure 2.** Ischemic damage and relative frequencies of nuclear morphologies. **A.** The percentage of ischemic pyramidal cells relative to the sum of intact and ischemic neurons within each survival group. This represents  $66.5 \pm 14.9\%$  at day 7. In **(B)** the percentage of ischemic pyramidal cells within each survival group is calculated as a decrease in number of intact neurons ( $67.6 \pm 19.1\%$  at day 7) relative to counts in controls. **C.** The clearance of pyramidal cells is calculated in percent as the sum of intact and ischemic pyramidal cells in each survival group relative to the number of pyramidal cells in controls. **D.** The percentage of pyramidal cells with pyknotic nuclei is shown relative to the sum of pyknotic (**D**), apoptosis-like (**E**) and necrosis-like (**F**) neurons within each group of animals with 3 to 7 days survival. Thus, the sum of ischemic morphologies at day 3 in panels **D, E, F**, is  $30\% + 60\% + 10\% = 100\%$  and so on for the other survival groups. The percentage of neurons with apoptosis-like morphology is indicated in panel **E**. The percentage of neurons with necrosis-like morphology is indicated in panel **F**. Data in panel **A-C** are presented as mean  $\pm$  standard error, whereas data in panel **D-F** represent cumulative values from each survival group. d = days.

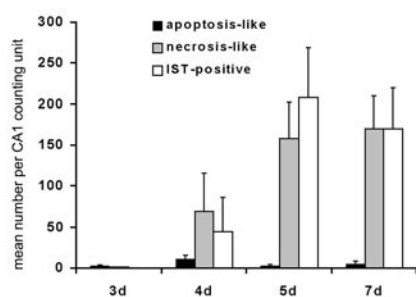


**Figure 3.** The incidence of apoptosis-like and necrosis-like morphologies in CA1 pyramidal cells as well as the incidence of IST-positive neurons are shown for groups of animals with 3 to 7 days survival. Data are presented as mean  $\pm$  standard error. (Counting unit  $\sim 1.66$  mm of the latero-medial extent of CA1). d = days.

incidence of IST-positive neurons. The ischemic CA1 damage and the relative distribution of neurons (in each survival group) with pyknotic, apoptosis-like death and necrosis-like death respectively are outlined in Figure 2.

By day 7 the overall extent of CA1 pyramidal cell death was  $67.6 \pm 19.1\%$  (Figure 2B).

**Expression of caspase-3 and ASP in ischemic hippocampus.** Caspase-3 and ASP immunostainings at 3 to 7 days after ischemia are illustrated in Figure 4 and their incidence per CA1 counting unit is seen in Figure 5A. Caspase-3/ASP immunoreactivity (IR) was detected in neurons

with apoptosis-like death and necrosis-like death. Pyknotic cell changes with caspase-3/ASP IR occurred at very low frequencies (data not shown). For both proteins, staining intensities were strongest at day 3 post-ischemia, when somata and neurites as well as nuclear components were strongly immunopositive (Figure 4). At day 4 post-ischemia, immunostaining of neuronal somata prevailed and immunopositive debris could be found in all layers of CA1. Occasionally, single nests of immunopositive debris could be identified 4 to 7 days after ischemia, possibly indicating phagocytosis of immunopositive material. At survival times 4 and 5 days, in parallel with an increasing frequency of necrosis-like death in CA1, the immunostainings became more faint. In general, the highest incidence of neurons positive for caspase-3 and ASP was found at day 4 (Figure 5A).

The number of caspase-3/ASP immunopositive neurons with nuclear apoptosis-like death (Figure 5B) or necrosis-like death (Figure 5C) relative to the number of cells with these respective nuclear changes in parallel H&E-stained sections showed the highest correlation at day 4 after ischemia. In general, high degrees of correlation occurred between the number of apoptosis-like neurons with caspase-3 IR and the number of neurons with apoptosis-like nuclear morphology in parallel H&E-stained sections (Figure 5B). The

correlation of neurons with necrosis-like death and caspase-3 was—except at day 4—significantly lower (Figure 5C). Of all the ischemic neurons found between day 1 to 7 in H&E-stained sections ( $n = 2607$ ), caspase-3 positive neurons with apoptosis-like death ( $n = 110$ ) comprised 4.2% as did caspase-3 positive neurons with necrosis-like death ( $n = 109$ ). Correspondingly, ASP positive neurons with apoptosis-like death ( $n = 89$ ) comprised 3.4% and ASP IR colocalized with necrosis-like death in 1.3% ( $n = 35$ ). In contrast, as aforementioned, classical apoptosis recognized by formation of apoptotic bodies was rarely found in the ischemic hippocampus, but those apoptotic bodies occasionally found were immunopositive for both apoptosis markers. Since there was no strong correlation between pyknosis and the markers of apoptosis, and pyknosis ( $n = 82$ ) only constituted 3.1% of all ischemic morphologies ( $n = 2607$ ) seen 1 to 7 days after ischemia in the H&E-stained sections, pyknotic neurons were not object for further analysis in our study.

The immunoreactivity of all PCD markers used in our study was also investigated in ischemic hilar neurons. No reactivity for caspase-3, ASP, or p-c-Jun was detected in hilar neurons of ischemic or sham-operated rats.

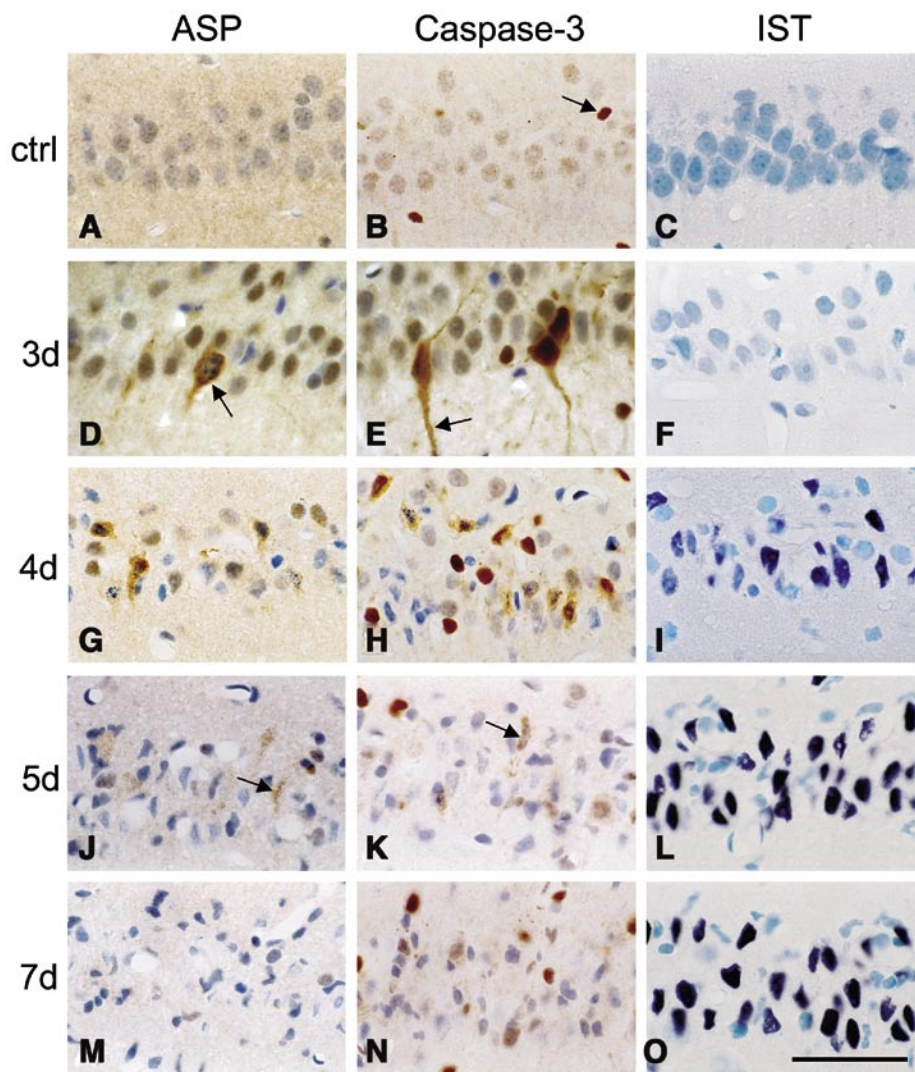


**Figure 4.** Immunohistochemistry for apoptosis specific protein (ASP, left column **A, D, G, J, M**), activated caspase-3 (middle column **B, E, H, K, N**) and in situ tailing (IST, right column **C, F, I, L, O**) in pyramidal cells of controls (ctrl, **A-C**) and animals with 3, 4, 5, 7 days survival. **A-C.** Sections from sham-operated rats show unspecific nuclear staining. Note, antibodies against both caspase-3 and ASP stain a small proportion of the nuclei unspecifically as exemplified by arrow in **B**. At 3 days, neurons with apoptosis-like morphology are strongly immunoreactive in their perikarya (arrow in **D**) and dendrites (arrow in **E**), but none of the neurons show IST staining (**F**). **G-I.** At 4 days, both apoptosis-like and necrosis-like morphologies could be seen with staining of the apoptosis markers located in their cytoplasm and IST staining emerged as well. **J-L.** At 5 days, necrosis-like morphologies are numerous and a small number of these show weak staining traces of the apoptosis markers (arrows in **J** and **K**). IST staining is increased both in number of neurons stained and staining intensity (**L**). **M-O.** At 7 days, stainings are as described 5 days after ischemia. Note, caspase-3 immunoreactivity was found in nuclei and perikarya at day 3. Bar: 50  $\mu$ m. d = days.

**Additional histopathological stainings.** In situ tailing for detection of DNA-fragmentation (Figure 3) showed that the nuclear morphologies with apoptosis-like death and necrosis-like death were IST-positive, whereas cells with pyknosis were IST-negative. Staining intensities for IST increased markedly from day 4 to day 5 after ischemia and peaked at day 7 (Figure 4). The strong nuclear IST-staining to some degree obscured identification of the underlying nuclear pathology such that only

total counts were obtained. Examination of the IST-negative nuclear pathologies in the sections revealed intact cells, pyknotic cells and a very small number of cells with apoptosis-like death, which was lower than the number of apoptosis-like cells in corresponding parallel H&E- stained sections (data not shown). The incidence of IST-positive neurons after ischemia is shown in Figure 3. Note that the IST-staining at day 3 to 4 underestimates the number of ischemic neurons, an effect that is equalized at

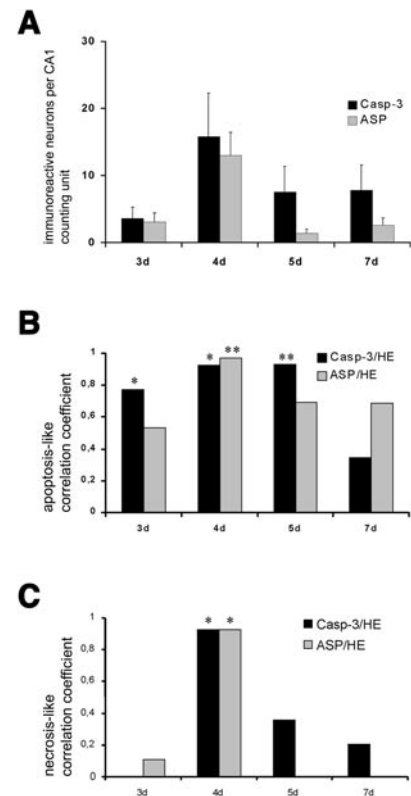


**Figure 5. A.** The incidence of caspase-3 IR and ASP IR in pyramidal cells at 3, 4, 5, 7 days survival. **B.** The correlation between the number of apoptosis-like CA1 neurons immunostained for apoptosis markers and the number of neurons with apoptosis-like morphology in the parallel HE stained sections is indicated. **C.** The correlation between the number of necrosis-like morphologies immunostained for apoptosis markers and the number of CA1 neurons with necrosis-like morphology in the parallel HE stained sections is indicated. Data in **A** are presented as mean  $\pm$  standard error. In **B-C** a significant correlation is indicated by asterisk as calculated from the Spearman Rank Order Test (\*,  $p < 0.05$ ; \*\*,  $p < 0.01$ ). Note, that in general caspase-3 recognized the apoptosis-like morphology best except at day 4 after ischemia when both markers recognized both the apoptosis-like and the necrosis-like morphologies. (Counting unit  $\sim 1.66$  mm of the latero-median extent of CA1; d = days).

day 7, indicating that early apoptoses either show minimal DNA fragmentation or lie below detection levels in our experiments.

Sections immunostained for detection of astrocytosis (GFAP antibody) or activated microglia (ED1 antibody) showed that the gliosis indicated by these two markers occurred simultaneously at day 4 to 7 after ischemia in parallel with the occurrence of IST-positive neurons and became strongest at day 7 post-ischemia (data not shown).

Immunohistochemical stainings for identification of neuronal serum albumin accumulation were negative in CA1 during

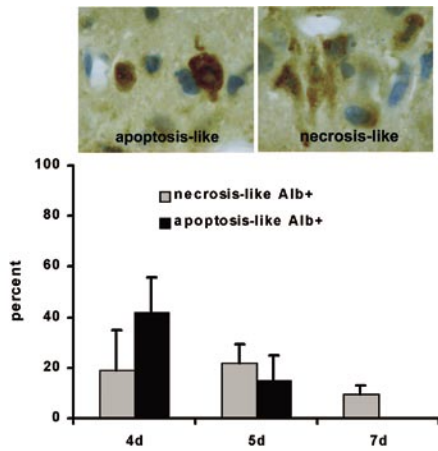


**Figure 6.** Intracellular serum albumin accumulation was found in ischemic pyramidal cells with apoptosis-like and necrosis-like morphologies on days 4 to 7. In brains with extravasated albumin, the percentage of the apoptosis-like morphologies with albumin IR was highest on day 4 ( $41.9 \pm 14\%$ ), whereas the percentage of the necrosis-like morphologies with albumin IR was highest on day 5 ( $22 \pm 7.2\%$ ). Micrographs show apoptosis- and necrosis-like CA1 neurons with albumin IR. Data are presented as mean  $\pm$  standard error. (d = days).

the first 3 days after ischemia. At days 4 to 7 days after the insult,  $41.9 \pm 14\%$  (day 4) and  $15 \pm 10\%$  (day 5) of all apoptosis-like and  $18.8 \pm 16\%$  (day 4),  $22 \pm 7.2\%$  (day 5) and  $9.4 \pm 3.4\%$  (day 7) of all necrosis-like neurons from animals with extravasated albumin showed somatic and neuritic albumin accumulation. The albumin staining was qualitatively most intense at day 4 (Figure 6). Efforts to further establish a time course for the extravasation of albumin into the neuropil were inconclusive as the breakdown of the blood brain barrier in the ischemic hippocampus is transient. Thus, the number of albumin immunoreactive CA1 neurons may underestimate the number of neurons with damaged plasma membranes.

Sections immunostained for p-c-Jun showed that CA1 neurons in control sections were immunonegative, whereas p-c-Jun immunopositive cells selectively appeared in ischemic CA1 neurons with intact nuclear morphology. Single CA3, but no hilar neurons were p-c-Jun immunopositive after ischemia. The highest incidence of p-c-Jun immunopositive neurons was found at day 3 post-ischemia and, roughly estimated, the total number of p-c-Jun positive neurons observed during 1 to 7 days after ischemia corresponded to the total number of neurons that later

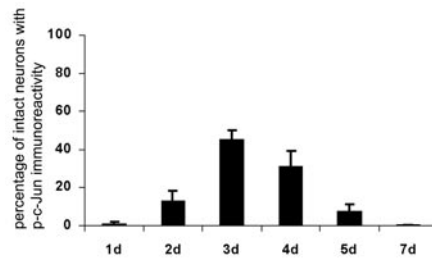


**Figure 7.** P-c-Jun IR could only be seen in CA1 neurons with intact morphology in ischemic animals at 1 to 7 days after ischemia. The percentage of intact neurons that contained p-c-Jun IR within the ischemic survival groups is shown. The highest frequency of p-c-Jun IR neurons was found on day 3, when  $45.2 \pm 4.9\%$  of all neurons with intact nuclei showed p-c-Jun IR. Data are presented as mean  $\pm$  standard error. (d = days).

succumbed to ischemia (Figure 7). In total, we found 2,599 p-c-Jun positive neurons in our material between 1 to 7 days post-ischemia, which corresponds well to the number of ischemic neurons found ( $n = 2607$ ).

Other parallel sections were silver stained for detection of the nucleolar morphology and the number of neurons with presence or absence of nucleoli was counted in normal neurons from control sections (Figure 8) and apoptosis-like or necrosis-like neurons from sections at day 3 to 7 after ischemia (Figure 8). The majority of neurons ( $79.8 \pm 6.6\%$ ) with apoptosis-like death had lost their nucleoli, whereas neurons with necrosis-like nuclear morphology ( $83.4 \pm 3.6\%$ ) contained preserved nucleoli to the same extent as did intact neurons in control sections ( $88.7 \pm 1\%$ ).

**Electron microscopy.** Ultrastructurally apoptosis-like changes in the neurons encompassed shrinkage and condensation of chromatin in the irregularly shaped nuclei. The plasma membrane and the nuclear envelope appeared intact (Figure 9). Some mitochondria were slightly dilated but otherwise showing a normal morphology. The rough endoplasmic reticulum and the free ribosomes were well preserved (Figure 9). Necrosis-like neurons were characterized by their highly fragmented chromatin lumps and showed disruption of plasmalemma and nuclear envelope. Their cytoplasm contained numerous vesicles.

## DISCUSSION

*Apoptosis-like death in ischemic hippocampus.* We have investigated the colo-

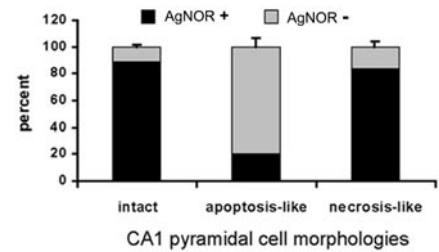


**Figure 8.** The percentage of pyramidal cells with (AgNOR+) and without (AgNOR-) nucleoli was estimated in neurons from control animals (intact) and ischemic animals (apoptosis-like and necrosis-like) at 3 to 7 days after ischemia. Most intact neurons ( $88.7 \pm 1\%$ ) in sections from control animals contained at least one nucleolus. The majority ( $79.8 \pm 6.6\%$ ) of the apoptosis-like morphologies had lost their nucleoli. In contrast,  $83.4 \pm 3.6\%$  of the necrosis-like morphologies had preserved nucleoli. Data are presented as mean  $\pm$  standard error AgNOR+/AgNOR- in each animal) from ischemia time points 3 to 7 days and from control animals. (AgNOR = silver staining for nucleolar organizer regions).

calization of defined LM nuclear ischemic changes with immunohistochemical apoptosis markers to identify apoptosis-like and necrosis-like death in ischemic hippocampus. Ischemic neuronal death occurred in CA1 pyramidal cells and in hilar neurons. Results showed that 4.2% of all ischemic neurons counted in CA1 hippocampus throughout the first 7 post-ischemic days showed apoptosis-like nuclear changes—that could be described as apoptosis-like death (36, 41)—in parallel with activated caspase-3. Although these ischemic neurons constitute a minority of the vulnerable CA1 neurons they could, by combining the nuclear morphology with the specific apoptosis markers, readily be identified. In support of our observation, previous studies have shown that cytoplasmic redistribution of cytochrome c occurred in a minority of ischemic CA1 pyramidal cells (60). We believe that these neurons correspond to a small portion of ischemic CA1 neurons previously identified in the EM by Zeng and Xu (59). Briefly, they found that at 48 hours post-ischemia a small portion of neurons contained shrunken invaginated nuclei with aggregated chromatin clumps. Swollen organelles were absent in these neurons. At later time points the chromatin aggregation broke into smaller particles but some neurons still displayed large clumps of chromatin with round or ovoid contours. Progressive loss of nucleolemmal integrity was reported, with consequent leakage of some electron dense chromatin

clumps into the cytoplasm; mitochondria and rough endoplasmic reticulum were slightly dilated. Up to 7 days after ischemia, neurons with small chromatin aggregations could occasionally be found in CA1. These observations are in agreement with our findings and the temporal profile of apoptosis-like neurons identified in our study. Our electron micrograph of a CA1 pyramidal cell with apoptosis-like morphology at 72 hours post-ischemia showed shrinkage and a characteristic irregular shape of the nucleus with condensed “clumped” nuclear chromatin surrounded by an intact nuclear envelope. The plasma membrane was intact, some mitochondria were slightly dilated but otherwise showing a normal morphology. The rough endoplasmic reticulum and the free ribosomes were well-preserved and a few membrane bound empty vacuoles were found in the cytoplasm. Indeed, the morphology of neuronal death at this stage could reflect a transient stage of caspase-dependent apoptosis, an aborted form of caspase-dependent apoptosis, or a caspase-independent form of death. Furthermore, caspase-3 can be activated during caspase-independent PCD without playing the role of the cell death executioner (15). Zeng et al (59) suggested that these ischemic CA1 neurons display major features of apoptosis quite different from the picture of necrosis. Furthermore, the same study pointed out that these dying apoptosis-like neurons have previously not been identified as apoptotic, probably because no apoptotic bodies were found. This is in agreement with our study where the occurrence of apoptotic bodies was extremely rare. Apoptotic bodies may not have been found in CA1 ischemia, because another form of programmed cell death—possibly caspase-independent—without formation of apoptotic bodies may take place.

**Necrosis-like death in ischemic hippocampus.** We further found that the other half of the caspase-3 IR neurons identified in our study—which also constitutes 4.2% of all ischemic neurons counted in CA1 hippocampus throughout the first 7 post-ischemic days—displayed necrosis-like changes in parallel with immunoreactivity of activated caspase-3. These neurons may resemble later stages of the neurons described by Zeng et al (59) when the chromatin clumps break into small pieces

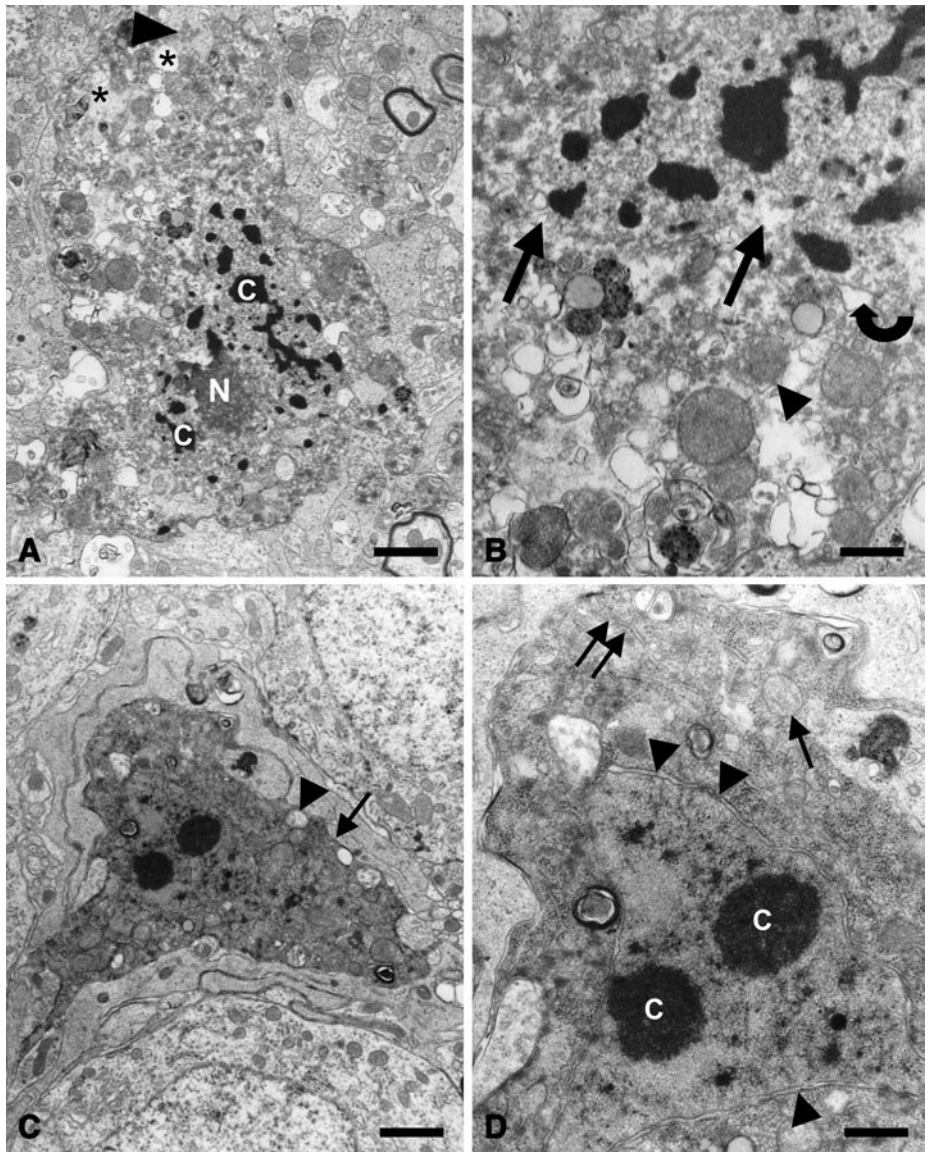


**Figure 9.** Electron microscopy of ischemic CA1 pyramidal cells. **A.** Electron micrograph of a necrosis-like ischemic CA1 neuron. The plasma membrane appears disrupted (arrowhead). Many large vesicles and empty spaces are found in the cytoplasm (asterisks), indicating swelling. The chromatin (C) is condensed into numerous irregular-shaped lumps. The nucleolus is well-defined (N). **B.** High magnification of the same necrosis-like cell. The nuclear envelope is not intact (arrows). Some mitochondria are lacking the characteristic double membrane structure (arrowhead). The rough endoplasmic reticulum appears dilated in some areas (curved arrow). **C.** Electron micrograph of an apoptosis-like CA1 pyramidal cell showing shrinkage and a characteristic irregular shape of nucleus. The plasma membrane appears intact (arrow). Few membrane bound empty vacuoles can be found in the cytoplasm (arrowhead). **D.** High magnification of the same apoptosis-like cell. Condensed chromatin (C) is seen in the nucleus surrounded by an intact nuclear envelope (arrowheads). In the cytoplasm well-developed rough endoplasmic reticulum (double arrow) and ribosomes can be observed, some well-preserved mitochondria are slightly dilated (arrow). Bars in **A** and **C**: 1  $\mu$ m; bars in **B** and **D**: 500 nm.

and the nucleolemma disappears with the result that small pieces of chromatin clumps are scattered in the cytoplasm (59). Alternatively, these neurons may not have passed the stage of apoptosis-like nuclear morphology but after activation of caspase-3 they may directly have turned into secondary necrosis-like morphology identified as chromatin segregation into innumerable speckles in our LM and

EM study. To test these 2 possibilities, we performed nucleolar stainings in parallel sections—the nucleolus is a substrate for activated caspase-3—and found that the vast majority of the apoptosis-like neurons had lost their nucleoli in contrast to the necrosis-like neurons that all had preserved their nucleoli. In apoptosis, the fate of the nucleoli is both tissue specific and related to the model and type of insult used (40).

Thus, in spontaneous apoptosis of thymocytes, nucleolar components can be recognized for a long time during the course of apoptosis (3). In other cell lineages undergoing apoptosis, nucleoli seem to progressively disappear and only rare nucleolar structures can be revealed in late apoptotic stages (9). In cisplatin-treated HeLa cells the segregation of nucleolar components coincides with caspase-3 activation (25). Since the necrosis-like neurons preserved their nucleoli, the apoptosis-like morphology is not a precursor to the necrosis-like morphology observed after ischemia, as it is unlikely that the nucleoli would re-emerge. Thus, ischemic caspase-3 IR cells with necrosis-like morphology probably suffer a caspase-3-aborted (preserved nucleoli) necrosis-like death characterized by chromatin fragmentation with or without formation of speckles.

*Activation of the c-Jun N-terminal kinase (JNK) pathway in ischemic CA1 pyramidal cells.* We estimated the number of cells with phosphorylation of c-Jun and found, in agreement with others (19, 42), that p-c-Jun IR became apparent after ischemia selectively in the vulnerable CA1 area. P-c-Jun IR was localized in nuclei of intact neurons in roughly the same number of neurons that later died from ischemia. Phosphorylation and translocation of c-Jun is a prerequisite for neuronal apoptosis in several models (1, 12, 22). C-Jun is selectively phosphorylated by phospho-JNK (30, 43).

There is increasing evidence that the JNK pathway plays an important role in cerebral ischemia. Inhibition of JNK with a peptide inhibitor decreases ischemic damage in a mouse MCAO model (4). The JNK3 isoform may, in particular, be responsible for mediating stress in neurons; mice deficient of this isoform show protection against focal ischemia (35). In ischemic CA1 pyramidal cells, activation of all JNK pathway components has been reported. Recently, a selective JNK inhibitor (AS601245) showed CA1 pyramidal cell protection in a model of global ischemia (6).

We suggest that the temporospatial and quantitative distribution of p-c-Jun IR in the ischemic hippocampus indicates early initiation of death programs in delayed CA1 pyramidal cell death. In terms of stroke therapy, the caspase-dependent

death constitutes up to 10% (4.2% caspase-dependent apoptosis-like death and 4.2% caspase-aborted necrosis-like death) of ischemic cell death in our study, whereas probably all ischemic cells share c-Jun phosphorylation and activation of the JNK pathway.

*Activation of cell death programs in neuronal injury and neurodegeneration.* Ischemic CA1 neuronal death appears to initially involve cell death programs as JNK (6) and caspase (5, 17, 23, 24) inhibitors may provide neuroprotection. Briefly, the studies by Chen et al (7), Gillardon et al (18), Himi et al (24) and Ni et al (44) support the idea of apoptosis in global ischemia, whereas studies by Colbourne et al (8), Deshpande et al (10), Li et al (37) and Zhan et al (60) argue against it. However, the caspase inhibitors used in most of these studies also block other proteases as cathepsin B and  $\mu$ calpain (49, 55), both of which have been suggested to mediate caspase-independent PCD in ischemic CA1 pyramidal cells (48, 57). Thus, the relative contribution of caspase-dependent and independent PCD to ischemic CA1 neuronal death remains to be determined. We suggest that activation of the JNK pathway with a resultant increase in p-c-Jun levels is a reliable marker for activation of the JNK pathway and for an upstream initiation of cell death programs in cerebral ischemia in general.

A role for PCD mechanisms has been suggested in many neurodegenerative diseases, such as Parkinson disease, Alzheimer disease, AIDS, prion diseases, amyotrophic lateral sclerosis, Huntington disease, dentatorubral pallidolusian atrophy, spinal bulbar muscular atrophy and spinocerebellar ataxias, as well as in head trauma (13, 21, 58). However, key questions in identification of PCD still concern the quantitation and the temporospatial course of PCD in these diseases. The guidelines outlined and the tools used in our LM study provide a practicable approach for this purpose. Controversies about PCD in global ischemia may be due to a small number of apoptosis-like neurons, which previously has been ignored. Only a small number of neurons with apoptotic and/or apoptosis-like morphology is visible at any one time point during progression of both physiological and pathological PCD; this is

supported by findings in Alzheimer disease, where only a very small number of neurons showed morphological features of apoptosis and caspase-3 expression (53, 54).

## CONCLUSIONS

We found that 4.2% of the ischemic CA1 cells succumb to a caspase-dependent apoptosis-like death characterized by chromatin condensation to lumpy compacted masses and another 4.2% of the ischemic CA1 cells die by caspase-aborted (preserved nucleoli) necrosis-like death characterized by chromatin dissolution into speckles. The rest and majority (91.6%) of the ischemic CA1 cells follows a caspase-independent necrosis-like death, characterized by chromatin fragmentation into speckles. All of these paradigms are likely to be preceded by activation of the JNK pathway and phosphorylation of c-Jun—followed or not by caspase-3 activation. Thus, ischemic CA1 pyramidal cell death comprises activation of cell death programs in the majority of neurons; however, at later times these programs are aborted resulting in secondary necrosis.

## ACKNOWLEDGMENTS

We would like to thank Lisbeth Thatt Jensen (Molecular Neuropathology Group, University of Copenhagen, Denmark), Marianne Leisser and Helene Breitschopf (both Brain Research Institute, Medical University of Vienna, Austria) for their excellent technical assistance. We would also like to thank Dr Marcel Leist (H. Lundbeck A/S, Valby, Denmark) for useful comments on the manuscript. Georg Johannes Müller was supported by a grant (Forschungsförderungsstipendium) from Medical University of Vienna. Christine Stadelmann is supported by the Gemeinnützige Hertie-Stiftung and the Medical Faculty of the University of Göttingen (junior research group). The study was financed by the Danish Medical Research Council (#22-02-0253), Mc-Kinney Møllers Foundation, Augustinus Foundation, Oda and Hans Svenningsens Foundation, Desiree and Nils Ydes Foundation, Ove William Buhl Olesens Foundation, Erna Hamilton Grant, Frimondts Foundation, Kong Christian den X's Foundation, Aase and Ejnar Danielsens Foundation, and P. Carl Petersens Foundation.



## REFERENCES

- Behrens A, Sibilina M, Wagner EF (1999) Amino-terminal phosphorylation of c-Jun regulates stress-induced apoptosis and cellular proliferation. *Nat Genet* 21: 326-329
- Bering R, Diemer NH, Draguhn A, Johansen FF (1995) Co-localization of somatostatin mRNA and parvalbumin in dorsal rat hippocampus after cerebral ischemia. *Hippocampus* 5: 341-348
- Biggiogera M, Bottone MG, Pellicciari C (1997) Nuclear ribonucleoprotein-containing structures undergo severe rearrangement during spontaneous thymocyte apoptosis. A morphological study by electron microscopy. *Histochem Cell Biol* 107: 331-336
- Borsello T, Clarke PG, Hirt L, Vercelli A, Repici M, Schorderet DF, Bogouslavsky J, Bonny C (2003) A peptide inhibitor of c-Jun N-terminal kinase protects against excitotoxicity and cerebral ischemia. *Nat Med* 9: 1180-1186
- Cao G, Luo Y, Nagayama T, Pei W, Stetler RA, Graham SH, Chen J (2002) Cloning and characterization of rat caspase-9: implications for a role in mediating caspase-3 activation and hippocampal cell death after transient cerebral ischemia. *J Cereb Blood Flow Metab* 22: 534-546
- Carboni S, Hiver A, Szyndralewicz C, Gaillard P, Gotteland JP, Vitte PA (2004) AS601245 (1,3-benzothiazol-2-yl (2-[[2-(3-pyridinyl) ethyl] amino]-4-pyrimidinyl) acetonitrile): a c-Jun NH2-terminal protein kinase inhibitor with neuroprotective properties. *J Pharmacol Exp Ther* 310: 25-32
- Chen J, Nagayama T, Jin K, Stetler RA, Zhu RL, Graham SH, Simon RP (1998) Induction of caspase-3-like protease may mediate delayed neuronal death in the hippocampus after transient cerebral ischemia. *J Neurosci* 18: 4914-4928
- Colbourne F, Sutherland GR, Auer RN (1999) Electron microscopic evidence against apoptosis as the mechanism of neuronal death in global ischemia. *J Neurosci* 19: 4200-4210
- Columbaro M, Gobbi P, Renò F, Luchetti F, Santi S, Valmori A, Falcieri E (1999) A multiple technical approach to the study of apoptotic cell micronuclei. *Scanning* 8: 541-548
- Desphande JK, Bergstedt K, Lindén T, Kalimo H, Wieloch T (1992) Ultrastructural changes in the hippocampal CA1 region following transient cerebral ischemia: evidence against programmed cell death. *Exp Brain Res* 88: 91-105
- Endres M, Namura S, Shimizu-Sasamata M, Waeber C, Zhang L, Gómez-Isla T, Hyman BT, Moskowitz MA (1998) Attenuation of delayed neuronal death after mild focal ischemia in mice by inhibition of the caspase family. *J Cereb Blood Flow Metab* 18: 238-247
- Estus S, Zaks WJ, Freeman RS, Gruda M, Bravo R, Johnson EM Jr (1994) Altered gene expression in neurons during programmed cell death: identification of c-jun as necessary for neuronal apoptosis. *J Cell Biol* 127: 1717-1727
- Evert BO, Wullner U, Klockgether T (2000) Cell death in polyglutamine diseases. *Cell Tissue Res* 301: 189-204
- Ferrer I, Pozas E, Marti M, Blanco R, Planas AM (1997) Methyl-azoxymethanol acetate-induced apoptosis in the external granule layer of the developing cerebellum of the rat is associated with strong c-Jun expression and formation of high molecular weight c-Jun complexes. *J Neuropathol Exp Neurol* 56: 1-9
- Foghsgaard L, Wissing D, Mauch D, Lademann U, Bastholm L, Boes M, Elling F, Leist M, Jäättelä M (2001) Cathepsin B acts as a dominant execution protease in tumor cell apoptosis induced by tumor necrosis factor. *J Cell Biol* 153: 999-1010
- Garrah JM, Bisby MA, Rossiter JP (1998) Immunolabelling of the cytoplasm and processes of apoptotic facial motoneurons following axotomy in the neonatal rat. *Acta Neuropathol* 95: 223-228
- Gillardon F, Kiprianova I, Sandkühler J, Hossmann K-A, Spranger M (1999) Inhibition of caspases prevents cell death of hippocampal CA1 neurons, but not impairment of hippocampal long-term potentiation following global ischemia. *Neuroscience* 93: 1219-1222
- Gillardon F, Böttiger B, Schmitz B, Zimmermann M, Hossmann KA (1997) Activation of CPP-32 protease in hippocampal neurons following ischemia and epilepsy. *Mol Brain Res* 50: 16-22
- Gillardon F, Spranger M, Tiesler C, Hossmann KA (1999) Expression of cell death-associated phospho-c-Jun and p53-activated gene 608 in hippocampal CA1 neurons following global ischemia. *Mol Brain Res* 73: 138-143.
- Gold R, Schmid M, Giegerich G, Breitschopf H, Hartung HP, Toyka KV, Lassmann H (1994) Differentiation between cellular apoptosis and necrosis by combined use of in situ tailing and nick translation techniques. *Lab Invest* 71: 219-225
- Gorman AM, Ceccatelli S, Orrenius S (2000) Role of mitochondria in neuronal apoptosis. *Dev Neurosci* 22: 348-358
- Ham J, Eilers A, Whitfield J, Neame SJ, Shah B (2000) c-Jun and the transcriptional control of neuronal apoptosis. *Biochem Pharmacol* 60, 1015-1021
- Han BH, Xu D, Choi J, Han Y, Xanthoudakis S, Roy S, Tam J, Vaillancourt J, Colucci J, Siman R, Giroux A, Robertson GS, Zamboni R, Nicholson DW, Holtzman DM (2002) Selective, reversible caspase-3 inhibitor is neuroprotective and reveals distinct pathways of cell death after neonatal hypoxic-ischemic brain injury. *J Biol Chem* 277: 30128-30136
- Himi T, Ishizaki Y, Murota S (1998) A caspase inhibitor blocks ischaemia-induced delayed neuronal death in the gerbil. *Eur J Neurosci* 10: 777-781
- Horky M, Wurzer G, Kotala V, Anton M, Vojtesek B, Vacha J, Wesierska-Gadek J (2001) Segregation of nucleolar components coincides with caspase-3 activation in cisplatin-treated HeLa cells. *J Cell Sci* 114: 663-670
- Horn M, Schlote W (1992) Delayed neuronal death and delayed neuronal recovery in the human brain following global ischemia. *Acta Neuropathol* 85: 79-87
- Ito U, Spat M, Walker JT Jr, Klatzo I (1975) Experimental cerebral ischemia in Mongolian gerbils: I. Light microscopic observations. *Acta Neuropathol* 32: 209-233
- Jäättelä M, Tschopp J (2003) Caspase-independent cell death in T lymphocytes. *Nat Immunol* 4: 416-423
- Johansen FF (1993) Interneurons in rat hippocampus after cerebral ischemia. Morphometric, functional, and therapeutic investigations. *Acta Neurol Scand Suppl* 150: 1-32
- Kallunki T, Su B, Tsigelny I, Sluss HK, Derijard B, Moore G, Davis R, Karin M (1994) JNK2 contains a specificity-determining region responsible for efficient c-Jun binding and phosphorylation. *Genes Dev* 8: 2996-3007
- Keane RW, Srinivasan A, Foster LM, Testa MP, Ord R, Nonner D, Wang HG, Reed JC, Bredesen DE, Kayalar C (1997) Activation of CPP32 during apoptosis of neurons and astrocytes. *J Neurosci Res* 48: 168-180
- Kerr JFR, Wyllie AH, Currie AR (1972) Apoptosis: a basic biological phenomenon with wide-ranging implications in tissue kinetics. *Br J Cancer* 26: 239-257
- Kirino T (1982) Delayed neuronal death in the gerbil hippocampus following ischemia. *Brain Res* 239: 57-69
- Kirino T, Sano K (1984) Selective vulnerability in the gerbil hippocampus following transient ischemia. *Acta Neuropathol* 62: 201-208
- Kuan CY, Whitmarsh AJ, Yang DD, Liao G, Schloemer AJ, Dong C, Bao J, Banasiak KJ, Haddad GG, Flavell RA, Davis RJ, Rakic P (2003) A critical role of neural-specific JNK3 for ischemic apoptosis. *Proc Natl Acad Sci U S A* 100: 15184-15189
- Leist M, Jäättelä M (2001) Four deaths and a funeral: from caspases to alternative mechanisms. *Nat Rev Mol Cell Biol* 2: 589-598
- Li H, Colbourne F, Sun P, Zhao Z, Buchan AM, Iadecola C (2000) Caspase inhibitors reduce neuronal injury after focal but not global ischemia in rats. *Stroke* 31: 176-182
- Lindner LE (1993) Improvements in the silver-staining technique for nucleolar organizer regions (AgNOR). *J Histochem Cytochem* 41: 439-445
- Lockshin RA, Zakeri Z (2001) Programmed cell death and apoptosis: origins of the theory. *Nat Rev Mol Cell Biol* 2: 545-550
- Martelli AM, Robuffo I, Bortol R, Ochs RL, Luchetti F, Cocco L, Zweyer M, Bareggi R, Falcieri E (2000) Behavior of nucleolar proteins during the course of apoptosis in camptothecin-treated HL60 cells. *J Cell Biochem* 78: 264-277
- Mathiasen IS, Jäättelä M (2002) Triggering caspase-independent cell death to combat cancer. *Trends Mol Med* 8: 212-220
- Matsuoka Y, Okazaki M, Zhao H, Asai S, Ishikawa K, Kitamura Y (1999) Phosphorylation of c-Jun and its localization with heme oxygenase-1 and cyclooxygenase-2 in CA1 pyramidal neurons after transient forebrain ischemia. *J Cereb Blood Flow Metab* 19: 1247-1255

43. Minden A, Lin A, Smeal T, Derijard B, Cobb M, Davis R, Karin M. (1994) c-Jun N-terminal phosphorylation correlates with activation of the JNK subgroup but not the ERK subgroup of mitogen-activated protein kinases. *Mol Cell Biol* 14: 6683-6688
44. Ni B, Wu X, Su Y, Stephenson D, Smalstig EB, Clemens J, Paul SM (1998) Transient global forebrain ischemia induces a prolonged expression of the caspase-3 mRNA in rat hippocampal CA1 pyramidal neurons. *J Cereb Blood Flow Metab* 18: 248-256
45. Nitatori T, Sato N, Waguri S, Karasawa Y, Araki H, Shibana K, Kominami E, Uchiyama Y (1995) Delayed neuronal death in the CA1 pyramidal cell layer of the gerbil hippocampus following transient ischemia is apoptosis. *J Neurosci* 15: 1001-1011
46. Petit CK, Feldmann E, Pulsinelli WA, Plum F (1987) Delayed hippocampal damage in humans following cardiorespiratory arrest. *Neurology* 37: 1281-1286
47. Pulsinelli WA, Brierley JB, Plum F (1982) Temporal profile of neuronal damage in a model of transient forebrain ischemia. *Ann Neurol* 11: 491-499
48. Rami A, Agarwal R, Botez G, Winckler J (2000) mu-Calpain activation, DNA fragmentation, and synergistic effects of caspase and calpain inhibitors in protecting hippocampal neurons from ischemic damage. *Brain Res* 866: 299-312
49. Schotte P, Declercq W, Van Huffel S, Vandenaabeele P, Beyaert R (1999) Non-specific effects of methyl ketone peptide inhibitors of caspases. *FEBS Lett* 442: 117-121
50. Smith M-L, Bendek G, Dahlgren N, Rosen I, Wieloch T, Siesjö BK (1984) Models for studying long-term recovery following forebrain ischemia in the rat. A 2-vessel occlusion model. *Acta Neurol Scand* 69: 385-401
51. Srinivasan A, Roth KA, Sayers RO, Shindler KS, Wong AM, Fritz LC, Tomaselli K (1998) In situ immunodetection of activated caspase-3 in apoptotic neurons in the developing nervous system. *Cell Death Differ* 5: 1004-1016
52. Stadelmann C, Mews I, Srinivasan A, Deckwerth TL, Lassmann H, Brück W (2001) Expression of cell death-associated proteins in neuronal apoptosis associated with pontosubicular neuron necrosis. *Brain Pathol* 11: 273-281
53. Stadelmann C, Brück W, Bancher C, Jellinger K, Lassmann H (1998) Alzheimer disease: DNA fragmentation indicates increased neuronal vulnerability, but not apoptosis. *J Neuropathol Exp Neurol* 5: 456-464
54. Stadelmann C, Deckwerth TL, Srinivasan A, Bancher C, Brück W, Jellinger K, Lassmann H (1999) Activation of caspase-3 in single neurons and autophagic granules of granulovacuolar degeneration in Alzheimer's disease. *Am J Pathol* 155: 1459-1466
55. Vancompernelle K, Van Herreweghe F, Pynaert G, Van de Craen M, De Vos K, Totty N, Sterling A, Fiers W, Vandenaabeele P, Grooten J (1998) Atractyloside-induced release of cathepsin B, a protease with caspase-processing activity. *FEBS Lett* 438: 150-158
56. Wyllie AH, Kerr JFR, Currie AR (1980) Cell death: the significance of apoptosis. *Int Rev Cytol* 68: 251-306
57. Yamashima T (2000) Implications of cysteine proteases calpain, cathepsin and scaspse in ischemic neuronal death of primates. *Progress Neurobiol* 62: 273-295
58. Yuan J, Yankner BY (2000) Apoptosis in the nervous system. *Nature* 407: 802-809
59. Zeng Y-S, Xu Z-C (2000) Co-existence of necrosis and apoptosis in rat hippocampus following transient forebrain ischemia. *Neurosci Res* 37: 113-125
60. Zhan R-Z, Wu C, Fujihara H, Taga K, Qi S, Naito M, Shimoji K (2001) Both caspase dependent and caspase-independent pathways may be involved in hippocampal CA1 neuronal death because of loss of cytochrome c from mitochondria in a rat forebrain ischemia model. *J Cereb Blood Flow Metabol* 21: 529-540